Intrinsic state lifetimes in ^{103}Pd and ^{106,107}Cd

S. F. Ashley,[1,2,*] P. H. Regan,[1] K. Andgren,[1,3] E. A. McCutchan,[2] N. V. Zamfir,[2,4,5] L. Amon,[2,6] R. B. Cakirli,[2,6] R. F. Casten,[2] R. M. Clark,[7] W. Gelletly,[1] G. Gürdal,[2,5] K. L. Keyes,[8] D. A. Meyer,[2,9] M. N. Erduran,[6] A. Papenberg,[8] N. Pietralla,[10,11] C. Plettner,[2] G. Rainovski,[10,12] R. V. Ribas,[13] N. J. Thomas,[1,2] J. Vinson,[2] D. D. Warner,[14] V. Werner,[2] E. Williams,[2] H. L. Liu,[15] and F. R. Xu[15]

[1]*Department of Physics, University of Surrey, Guildford GU2 7XH, United Kingdom*
[2]*Wright Nuclear Structure Laboratory, Yale University, New Haven, Connecticut 06520, USA*
[3]*Department of Physics, Royal Institute of Technology, S-10405 Stockholm, Sweden*
[4]*Institutul Naţional de Fizică şi Inginerie Nucleară, RO-76900 Bucureşti-Măgurele, Romania*
[5]*Clark University, Worcester, Massachusetts 01610-1477, USA*
[6]*Department of Physics, Istanbul University, Istanbul, Turkey*
[7]*Lawrence Berkeley National Laboratory, Berkeley, California 94720, USA*
[8]*Institute of Physical Research, University of Paisley, Paisley PA1 2BE, United Kingdom*
[9]*Department of Physics, Rhodes College, Memphis, Tennessee 38112, USA*
[10]*Department of Physics and Astronomy, SUNY, Stony Brook, New York 11794, USA*
[11]*Institut für Kernphysik, Technische Universität Darmstadt, D-64289 Darmstadt, Germany*
[12]*Faculty of Physics, St. Kliment Ohridski University of Sofia, Sofia 1164, Bulgaria*
[13]*Instituto de Física, Universidade de São Paulo, São Paulo, SP, 05315-970, Brazil*
[14]*Council for the Central Laboratory of the Research Councils, Daresbury Laboratory, Daresbury, Warrington WA4 4AD, United Kingdom*
[15]*School of Physics, Peking University, Beijing 100871, People's Republic of China*

(Received 4 September 2007; revised manuscript received 21 October 2007; published 4 December 2007)

The mean-lifetimes, τ, of various medium-spin excited states in ^{103}Pd and ^{106,107}Cd have been deduced using the Recoil Distance Doppler Shift technique and the Differential Decay Curve Method. In ^{106}Cd, the mean-lifetimes of the $I^\pi = 12^+$ state at $E_x = 5418$ keV and the $I^\pi = 11^-$ state at $E_x = 4324$ keV have been deduced as 11.4(17)ps and 8.2(7)ps, respectively. The associated β_2 deformation within the axially-symmetric deformed rotor model for these states are 0.14(1) and 0.14(1), respectively. The β_2 deformation of 0.14(1) for the $I^\pi = 12^+$ state in ^{106}Cd compares with a predicted β_2 value from total Routhian surface (TRS) calculations of 0.17. In addition, the mean-lifetimes of the yrast $I^\pi = \frac{15}{2}^-$ states in ^{103}Pd (at $E_x = 1262$ keV) and ^{107}Cd (at $E_x = 1360$ keV) have been deduced to be 31.2(44)ps and 31.4(17)ps, respectively, corresponding to β_2 values of 0.16(1) and 0.12(1) assuming axial symmetry. Agreement with TRS calculations are good for ^{103}Pd but deviate for that predicted for ^{107}Cd.

DOI: 10.1103/PhysRevC.76.064302 PACS number(s): 21.10.Tg, 23.20.Lv, 25.70.Gh, 27.60.+j

I. INTRODUCTION

Gamma-ray spectroscopy of the excited states within cadmium and palladium isotopes have yielded interesting features associated with the competition between vibrational and rotational collective excitation in nuclei [1–5] (and references therein). At higher spins within $^{106-110}$Cd, collective structures built upon two quasiparticle excited states, such as maximally aligned, decoupled $(\nu h_{\frac{11}{2}})^2$ bands built upon a $I^\pi = 10^+$ bandhead and other four and six quasiparticle structures in ^{106}Cd [6], ^{108}Cd [7,8], ^{110}Cd [9–11], and ^{112,114}Cd [12] are evident. References [13–15] suggest that from deduced intraband $B(E2)$ values, the collective excited states above the yrast $I^\pi = 16^+$ state in ^{106,108}Cd are generated by "antimagnetic rotation". Sequences built on the $\nu h_{\frac{11}{2}}$ orbital are a readily apparent feature in the odd-A cadmium [11,16] and palladium isotopes [17–20]. Initial comparative studies of the energetics of these bands in cadmium [16,21] and palladium isotopes [20,22] suggested that there is a rotation-aligned coupling (RAC) [23] of the unpaired neutron to the core states.

This paper reports on an experiment using a Recoil Distance Doppler Shift technique [24] to determine $B(E2)$ values of medium spin near-yrast states in ^{103}Pd and ^{106,107}Cd. Preliminary analyses of some of the results from this work have been presented in conference proceedings [25–27]. The values quoted in the present work vary with the values presented in [25,26] due to differences in the normalisation used and the uncertainty associated with the spread in recoil velocity (see Sec. II B).

II. EXPERIMENTAL DETAILS

A. Overview

Two experiments were undertaken at the Wright Nuclear Structure Laboratory, Yale University in August 2004. Both experiments used the ^{98}Mo(^{12}C, xn)$^{110-x}$Cd and ^{98}Mo(^{12}C, αxn)$^{106-x}$Pd fusion-evaporation reactions to populate medium-spin excited states in the nuclei of interest, with the ^{12}C beam, provided from the Yale ESTU Tandem Van de

*s.ashley@surrey.ac.uk

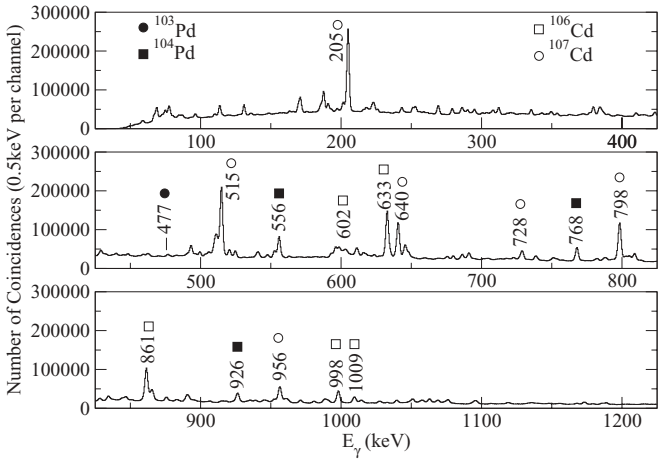

FIG. 1. Total projection of γ-γ coincidence matrix for the ^{98}Mo $+^{12}$ C reaction at 60 MeV using the backed target.

Graaff accelerator [28]. The beam had an average on-target current of 2 → 3 pnA and incident energy of 60 MeV in the laboratory frame. The reaction γ rays were detected using the SPEEDY γ-ray array [29] in a configuration with seven HPGe clover detectors, four of which were at angle of 41.5°, three of which were at an angle of 138.5°, relative to the beam-line axis. The data acquisition was set such that a valid event had to consist of two (or more) γ rays being detected within a 2 μs time window.

The first experiment was a backed target experiment consisting of a 0.5 mg/cm^2,^{98}Mo target on a 9 mg/cm^2 ^{197}Au backing and was primarily used for level scheme determination. From the total projection spectra shown in Fig. 1, it is apparent that excited states in ^{103,104}Pd and ^{106,107}Cd were populated in the current work. By investigating the coincident γ rays, partial level schemes of ^{103}Pd and ^{106,107}Cd, shown in Figs. 2 and 3, were constructed to show the excited states populated in this reaction. These level schemes are consistent with the previously reported level schemes for these nuclei, as published in Refs. [6,21,30].

The second experiment was a Recoil Distance Doppler Shift (RDDS) experiment [24] consisting of a 1.05 mg/cm^2, self-supporting ^{98}Mo target with a separate 10 mg/cm^2 ^{197}Au stopper. The quoted target thickness is an upper limit and was

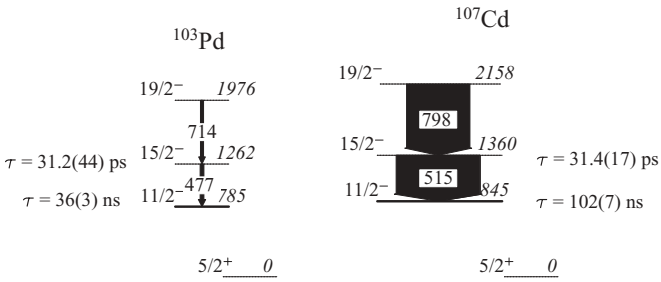

FIG. 2. Partial level schemes for ^{103}Pd and ^{107}Cd as observed in the backed-target data. The width of the arrows represents the relative intensity of the transitions observed in the γ-γ coincidence data. The mean-lieftimes of the $I^\pi = \frac{11}{2}^-$ in ^{103}Pd and ^{107}Cd were taken from [47] and [48].

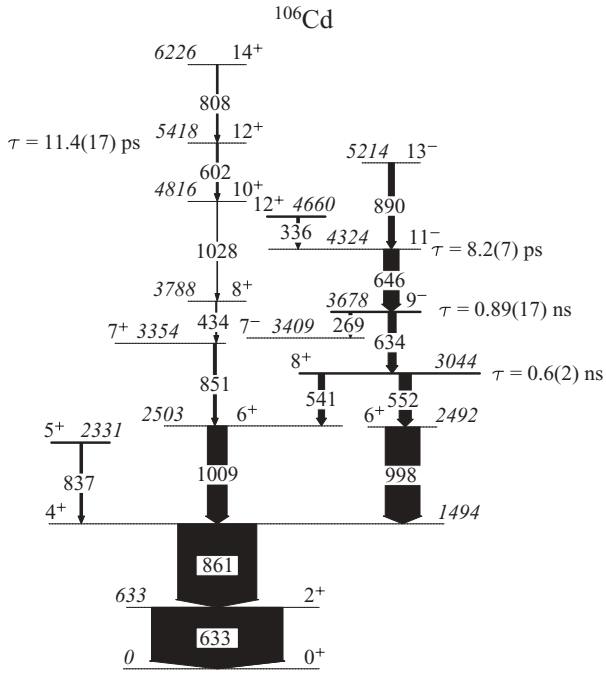

FIG. 3. Partial level scheme for ^{106}Cd as observed in the backed-target data. The width of the arrows represents the relative intensity of the transitions observed in the γ-γ coincidence data.

deduced from energy loss of α particles after the experiment [31]. For the latter experiment, the New Yale Plunger Device (NYPD) [32] was utilized to set and maintain the distance between the target and stopper. In total, ten distances, ranging from 11 μm to 2 mm were set, with the total number of $\gamma\gamma$ coincidences recorded at each distance given in Table I. The average $\gamma\gamma$ master rate for both experiments was 4 → 5 kHz. For each distance, the acquired data were sorted offline into three, two-dimensional E_γ- E_γ matrices, for forward ($\theta = 41.5°$) vs backward ($\theta = 138.5°$), forward vs forward, and backward vs backward detectors, respectively, with a 'prompt' time condition set such that two γ-rays had to be detected within ∼50 ns. The coincidence matrices were then subsequently analysed using the TV analysis software [33] as used in Refs. [34,35].

TABLE I. Number of coincidences recorded for each target-stopper distance.

Target-stopper distance (μm)	No. of coincidences ($\times 10^8$)
11	1.6
14	1.3
18	1.3
23	1.5
28	2.0
41	1.3
56	1.1
127	1.5
330	0.9
2008	0.8

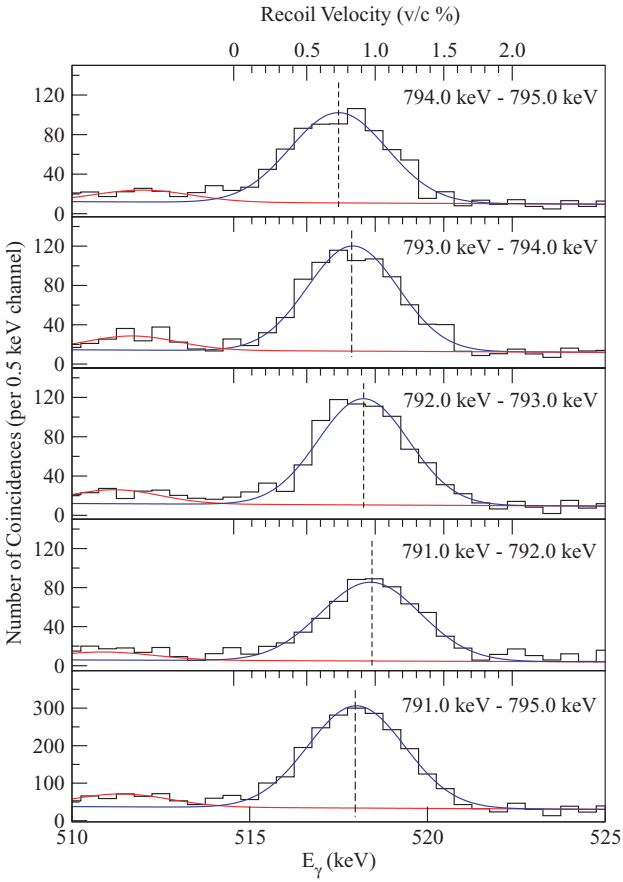

FIG. 4. (Color online) Projection of the forward-shifted 515 keV, $I^\pi = \frac{15}{2}^- \rightarrow \frac{11}{2}^-$ transition in ^{107}Cd from gating on the 798 keV, $I^\pi = \frac{19}{2}^- \rightarrow \frac{15}{2}^-$ transition. The target-stopper distance for these spectra is 330 μm. The range of the γ-ray coincidence condition is shown in the upper right corner of each spectrum. The dashed line denotes the measured centroid of the Doppler-shifted peak.

B. DDCM analysis and results

The differential decay curve method (DDCM) [36,37] is an analysis technique used for data obtained from Recoil Distance Doppler Shift experiments, such that mean-lifetimes of excited states in nuclei can be determined precisely. In the analysis of the current work, a γ-ray energy coincidence gate was placed on the Doppler-shifted component (for each distance) of the transition directly feeding the excited state of interest. Thereafter, the intensities of the stopped and Doppler-shifted γ rays for a transition depopulating this excited state were determined by fitting two Gaussian curves to these peaks. Each set of intensities for stopped and Doppler-shifted peaks was normalised such that the sum of these intensities are constant. This was performed by dividing each set of intensities by the number of counts in each projection spectrum. The mean-lifetime of this excited state could then be extracted directly using Eq. (1) (see [36] for a full derivation), where I_U and I_S are the respective intensities of stopped and shifted transitions, v is the recoil velocity, τ is the mean-lifetime of the excited state and x is the target-stopper distance. The NAPATAU program [38] was used to fit curves to the stopped and Doppler-shifted normalized intensities and also to deduce the mean-lifetime:

$$\tau = \frac{I_U}{v\frac{dI_s}{dx}}. \quad (1)$$

For standard DDCM analysis, the most significant errors associated with the measured mean-lifetime arise from the statistical uncertainties associated with the fitting of the decay curves and the range in the recoil velocities in the nuclei of interest. In the current work, there was a significant spread in recoil velocities due to the relatively low initial recoil velocity ($\frac{v}{c} \approx 1\%$) and the beam and recoils slowing down/stopping within the target. The low $\frac{v}{c}$ of the recoiling compound nucleus resulted in a small energy separation between the stopped and Doppler-shifted peaks. In some cases, only partial selection of the shifted component could be used as the feeding component and this in turn modifies the selection of recoil velocities. Previous works have accounted for this spread in recoil velocity by determining the velocity distribution of the recoils by Monte Carlo techniques and subsequent Doppler Shift Attenuation (DSA) measurements (see Ref. [39]). In the current analysis, repeated measurements of the lifetimes were performed by selecting "narrow" energy/velocity components of the feeding transition, along with a "wide" energy/velocity gate which covers the sum of the individual narrow energy/velocity components. This is demonstrated in Fig. 4, which shows the projections of the forward Doppler-shifted components of the 515 keV, $I^\pi = \frac{15}{2}^- \rightarrow \frac{11}{2}^-$ transition in ^{107}Cd. The upper four spectra are projections from four 1 keV wide backward-shifted gates, ranging from 791 keV to 795 keV and the bottom spectrum is the sum gate spanning from 791 keV to 795 keV. It is evident from Fig. 4 that there is a continuous displacement in peak position and thus recoil velocity from $\frac{v}{c} = 0.0080 \rightarrow 0.0096$. A systematic error has been incorporated for the spread of recoil velocities, which is added in quadrature to the statistical error. This systematic error is approximated to the range of recoil velocities for a single 1 keV wide gate in the total projection spectrum. The values of the statistical and systematic error are presented separately in the results section. The resultant value for the mean-lifetime comes from the weighted mean of the mean-lifetimes deduced from all "narrow" and "wide" gating combinations. Further details of the gating conditions used for each lifetime measurement, plus all spectra and decay curves, can be found in Ref. [40].

C. Lifetime determination of excited states in ^{106}Cd

1. *Lifetime determination of the $I^\pi = 12^+$ state at $E_x = 5418$ keV*

The mean-lifetime of the 5418 keV, $I^\pi = 12^+$ state, was determined by gating on the Doppler-shifted component of the 808 keV, $I^\pi = 14^+ \rightarrow 12^+$ transition and projecting the stopped and shifted components of the $I^\pi = 12^+ \rightarrow 10^+$ transition. An example of such a projection is shown in Fig. 5. A single 4 keV wide gate was placed on the forward-shifted component of the 808 keV, $I^\pi = 14^+ \rightarrow 12^+$ transition and a single 3 keV wide gate was placed on the backward-shifted component of the 808 keV, $I^\pi = 14^+ \rightarrow 12^+$ transition. From

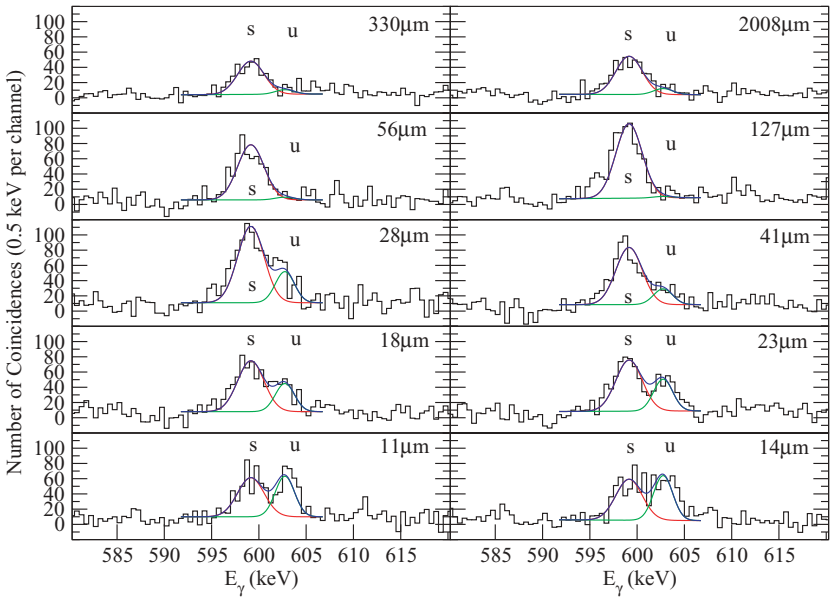

FIG. 5. (Color online) Projected stopped and backward-shifted components for the 602 keV, $I^\pi = 12^+ \rightarrow 10^+$ transition in ^{106}Cd from gating on the forward-shifted component of the 808 keV, $I^\pi = 14^+ \rightarrow 12^+$ transition, where u and s denote the unshifted and-shifted components, respectively.

deconvolution, fitting, and normalization of the stopped and shifted peaks, decay curves were determined for both summed forward and backward transitions. Thus, mean-lifetimes (with statistical errors) of 12.4(11) ps and 10.9(5) ps were deduced for forward and backward rings, respectively (see Fig. 6). The systematic errors due to the spread in recoil velocity for the forward and backward rings were 2.6 ps ($\frac{v}{c} = 0.0078$; $\frac{\Delta v}{c} = 0.0017$) and 2.0 ps ($\frac{v}{c} = 0.0078$; $\frac{\Delta v}{c} = 0.0014$), respectively.

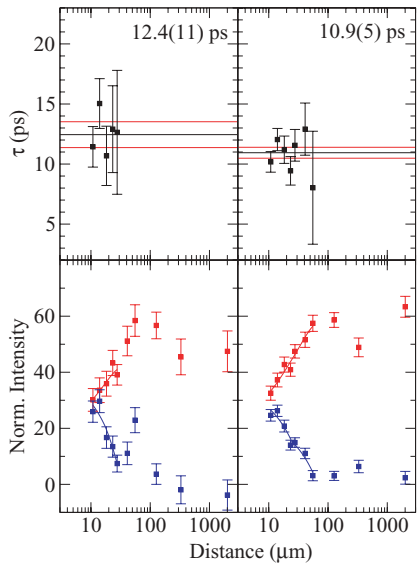

FIG. 6. (Color online) Decay curves and lifetime determinations of the 602 keV, $I^\pi = 12^+ \rightarrow 10^+$ transition in ^{106}Cd. The lower panel shows the stopped and Doppler-shifted intensities (in blue and red, respectively) vs distance. From fitting second-order polynomials to both the stopped and Doppler-shifted intensities shown by the blue and red lines, respectively, the mean-lifetime at each distance is determined [using Eq. (1)] and is shown in the upper panel as function of distance. The weighted average of these values yields the overall mean-lifetime.

Combining these values with the statistical uncertainties yielded mean-lifetimes values of the forward and backward rings of 12.4(29) ps and 10.9(21) ps, respectively. The resultant weighted mean value for the mean-lifetime of the $I^\pi = 12^+$ state is 11.4(17) ps.

2. *Lifetime determination of the $I^\pi = 11^-$ state at $E_x = 4324$ keV*

A similar technique, as described above, was performed for determining the lifetime of the $I^\pi = 11^-$ state at $E_x = 4324$ keV. A gate was placed on the forward-shifted component of the 890 keV, $I^\pi = 13^- \rightarrow 11^-$ transition, projecting the 646 keV, $I^\pi = 11^- \rightarrow 9^-$ transition in both forward and backward rings. The forward projection of a 4 keV wide gate on the feeding transition is shown in Fig. 7. From the resulting decay curves, the deduced mean-lifetime of the $I^\pi = 11^-$ state at $E_x = 4324$ keV is 8.2(7) ps.

D. Lifetime determination of the yrast $I^\pi = \frac{15}{2}^-$ state in ^{103}Pd and ^{107}Cd

1. *Lifetime determination of the $I^\pi = \frac{15}{2}^-$ state at $E_x = 1262$ keV in ^{103}Pd*

The lifetime of the yrast $I^\pi = \frac{15}{2}^-$ state at $E_x = 1262$ keV in ^{103}Pd was determined only by gating on the backward-shifted component of the populating 714 keV, $I^\pi = \frac{19}{2}^- \rightarrow \frac{15}{2}^-$ transition (the forward-shifted component was not used due to overlap with a coincident 718 keV γ ray from the $I^\pi = \frac{9}{2}^+ \rightarrow \frac{5}{2}^+$ transition in ^{103}Pd). A single 2.5 keV wide gate was placed on the feeding transition. The forward-shifted projection of the depopulating 477 keV, $I^\pi = \frac{15}{2}^- \rightarrow \frac{11}{2}^-$ transition is shown in Fig. 8. The resultant value for the mean-lifetime of the $I^\pi = \frac{15}{2}^-$ state at $E_x = 1262$ keV was deduced to be 31.2(44) ps.

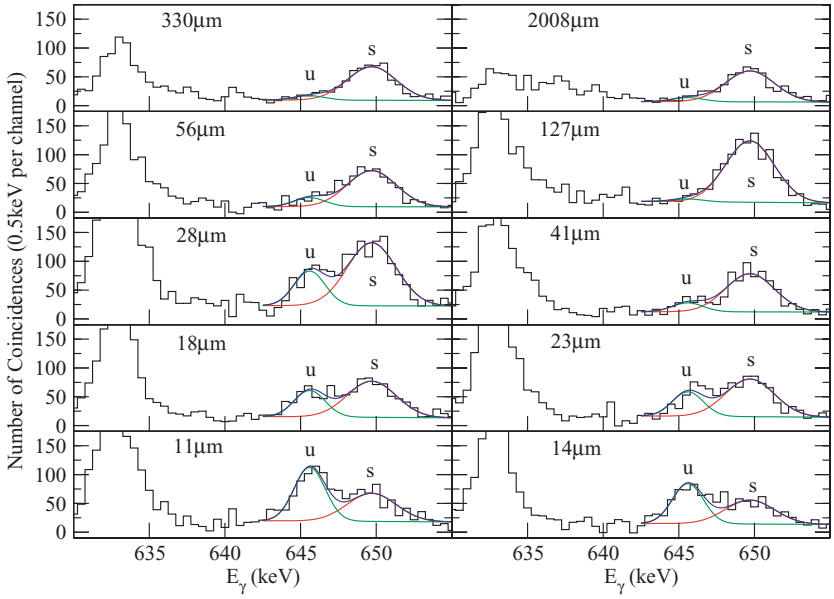

FIG. 7. (Color online) Projected stopped and forward-shifted components for the 646 keV, $I^\pi = 11^- \rightarrow 9^-$, transition in ^{106}Cd.

2. *Lifetime determination of the* $I^\pi = \frac{15}{2}^-$ *state at* $E_x = 1360$ keV *in* ^{107}Cd

The lifetime of the $I^\pi = \frac{15}{2}^-$ state in ^{107}Cd was determined by gating on the shifted component of the populating 798 keV, $I^\pi = \frac{19}{2}^- \rightarrow \frac{15}{2}^-$ transition. The forward-shifted gate, forward-shifted projection of the $I^\pi = \frac{15}{2}^- \rightarrow \frac{11}{2}^-$ transition is shown in Fig. 9. The resultant mean-lifetime of the $I^\pi = \frac{15}{2}^- \rightarrow \frac{11}{2}^-$ state at $E_x = 1360$ keV in ^{107}Cd is 31.4(17) ps.

III. DISCUSSION

The mean-lifetimes, τ can be converted into $B(E2)$ values using the formula in Eq. (2) [41]

$$B(E2) = \frac{1}{1.225 \times 10^9 E_\gamma^5 \tau (1+\alpha)}, \qquad (2)$$

where E_γ is the γ-ray energy (in MeV) of the $E2$ transition depopulating the decaying state, α is the total internal conversion coefficient, the mean-lifetime, τ, is in ps, and the $B(E2)$ values are in units of e^2fm^4. Cranked shell model calculations, reported in [6], suggest that the collective excitations built upon the $(\nu h_{\frac{11}{2}})^2$, $I^\pi = 10^+$ state at $E_x = 4812$ keV in ^{106}Cd are rotational and that the nucleus is weakly deformed. Similarly, the $\nu h_{\frac{11}{2}}$ configuration associated with the $I^\pi = \frac{11}{2}^-$ states in ^{103}Pd and ^{107}Cd is also assumed to be weakly deformed [21,22]. Therefore, the $B(E2)$ values can then be directly substituted into Eq. (3), assumed for an axially symmetric deformed nucleus [42], which yields a deformation in β_2:

$$B(E2) = \frac{5}{16\pi} e^2 Q_t^2 |\langle J_i K 20 | J_f K \rangle|^2, \qquad (3)$$

$$Q_t \approx \frac{3}{\sqrt{5\pi}} Z R_0^2 \beta_2 (1 + 0.16\beta_2), \qquad (4)$$

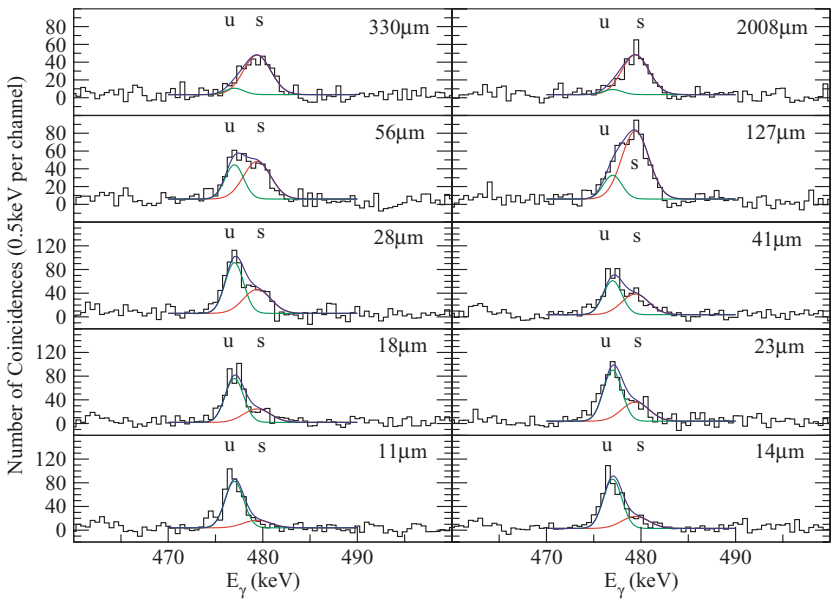

FIG. 8. (Color online) Projected stopped and forward-shifted components for the 477 keV, $I^\pi = \frac{15}{2}^- \rightarrow \frac{11}{2}^-$, transition in ^{103}Pd.

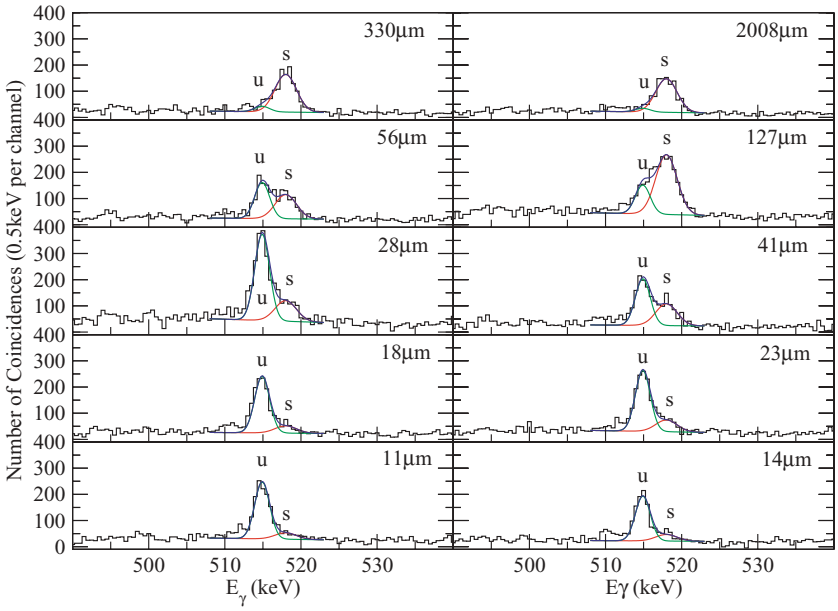

FIG. 9. (Color online) Projected stopped and forward-shifted components for the 515 keV, $I^\pi = \frac{15}{2}^- \rightarrow \frac{11}{2}^-$, transition in ^{107}Cd.

where Q_t is the transition quadrupole moment and R_0 is the average nuclear radius (given by $1.2A^{1/3}$ fm). Values of $K = 0$ for the $I^\pi = 12^+$ state in ^{106}Cd [6], $K = \frac{1}{2}$ for the $I^\pi = \frac{15}{2}^-$ states in ^{103}Pd and ^{107}Cd [16,18] and $K = 2$ for the $I^\pi = 11^-$ state in ^{106}Cd [6] have been assumed in the current analysis. The value of β_2, obtained from Eq. (4) is compared to values obtained from total Routhian surface (TRS) calculations [43].

A. $I^\pi = 12^+$ and $I^\pi = 11^-$ collective states in ^{106}Cd

The $B(E2)$ values of 30.4(45) W.u and 29.7(25) W.u. for the $I^\pi = 12^+$ and $I^\pi = 11^-$ states correspond to axially symmetric β_2 deformations of 0.14(1) and 0.14(1), respectively. TRS calculations [see (b) of Fig. 10], for the $I^\pi = 12^+$ state assuming a $(\nu h_{11/2})^2$ character, yield an associated β_2 deformation of 0.17.

B. $I^\pi = \frac{15}{2}^-$ states in ^{103}Pd and ^{107}Cd

The deduced β_2 deformation of 0.16(1) for the $I^\pi = \frac{15}{2}^-$ state in ^{103}Pd is consistent with the predicted value of 0.16 from the TRS calculation. The mean-lifetime of the $I^\pi = \frac{15}{2}^-$ state in ^{107}Cd obtained in the current work [31.4(17) ps] is significantly larger than the previously measured value for this state by Häusser *et al.* [44] of 23.5(15) ps. We note that the value reported by Häusser *et al.* did not use the coincidence-based DDCM to analyze the data and thus unobserved feeding effects could attribute for the measured difference. The deduced β_2 deformation of 0.12(1) for this state in ^{107}Cd, compares with the TRS prediction of 0.18. We note, however, that the deformation predicted for the ground state of ^{107}Cd by Möller-Nix ($\beta_2 = 0.135$) [45] is closer to the experimentally deduced β_2 value. Interestingly,

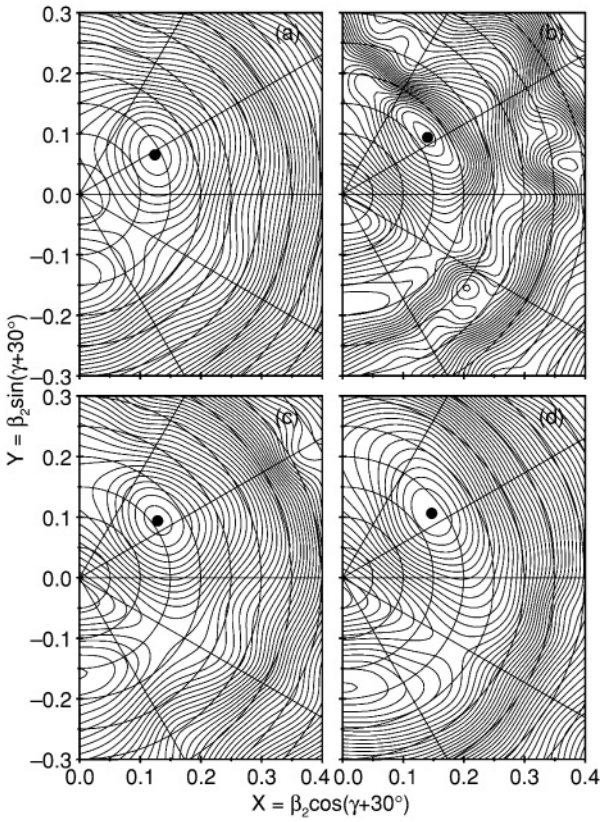

FIG. 10. Total Routhian surface calculations. (a) ^{106}Cd, (0,+) vacuum configuration; $\omega = 0.30$, $\beta_2 = 0.14$, $\gamma = -2.1°$, $I_x = 2.2\hbar$ and $\beta_4 = -0.01$. (b) ^{106}Cd, $(0,+)$ $(\nu h_{\frac{11}{2}})^2$ configuration; $\omega = 0.30$, $\beta_2 = 0.17$, $\gamma = 3.9°$, $I_x = 11.8\hbar$ and $\beta_4 = 0.01$. (c) ^{103}Pd, $(-\frac{1}{2},-)$ $\nu h_{\frac{11}{2}}$ configuration; $\omega = 0.25$, $\beta_2 = 0.16$, $\gamma = 6.2°$, $I_x = 7.2\hbar$ and $\beta_4 = 0.00$. (d) ^{107}Cd, $(-\frac{1}{2},-)$ $\nu h_{\frac{11}{2}}$ configuration; $\omega = 0.25$, $\beta_2 = 0.18$, $\gamma = 5.7°$, $I_x = 7.6\hbar$ and $\beta_4 = 0.02$.

TABLE II. Summary of the results deduced within this paper, where E_x is the excitation energy of the level, E_γ^{Pop} and $E_\gamma^{\mathrm{Depop}}$ is the energy of γ ray, populating and depopulating the level of interest, respectively, $I_i^\pi \rightarrow I_f^\pi$ denotes the spins and parities of the initial and final state and $\tau_{\mathrm{Meas}}^{\mathrm{Int}}$ is the measured intrinsic mean-lifetime of the state.

Nucleus	E_x	E_γ^{Pop}	$E_\gamma^{\mathrm{Depop}}$	$I_i^\pi \rightarrow I_f^\pi$	$\tau_{\mathrm{Meas}}^{\mathrm{Int}}$	$B(E2)$ $e^2\mathrm{fm}^4$	$B(E2)$ W.u.	β_2	β_2 (TRS)
^{106}Cd	5418 keV	808 keV	602 keV	$12^+ \rightarrow 10^+$	11.4(17) ps	906(135)	30.4(45)	0.14(1)	0.17
	4324 keV	890 keV	646 keV	$11^- \rightarrow 9^-$	8.2(7) ps	885(76)	29.7(25)	0.14(1)	N/A
^{103}Pd	1262 keV	714 keV	477 keV	$\frac{15}{2}^- \rightarrow \frac{11}{2}^-$	31.2(44) ps	1060(142)	37(5)	0.16(1)	0.16
^{107}Cd	1360 keV	798 keV	515 keV	$\frac{15}{2}^- \rightarrow \frac{11}{2}^-$	31.4(17) ps	718(39)	23.8(13)	0.12(1)	0.18

the mean-lifetime of the yrast $I^\pi = \frac{15}{2}^-$ state in ^{107}Cd from this measurement is a factor of two larger than the yrast $I^\pi = \frac{15}{2}^-$ state in ^{109}Cd [46]. The corresponding higher β_2 value of 0.18 in ^{109}Cd [46] suggests a larger deformation for the configuration in that nucleus compared to ^{107}Cd.

IV. SUMMARY AND CONCLUSIONS

In summary, an experiment has been performed using the Yale ESTU tandem Van de Graaff accelerator, SPEEDY γ-ray array, and New Yale Plunger Device to populate medium spin states in ^{103}Pd and ^{106,107}Cd. Utilizing the differential decay curve method, the mean-lifetimes of various excited states have been deduced and are presented in Table II. The inferred axially symmetric β_2 deformation of 0.14(1) for the $I^\pi = 12^+$ state in ^{106}Cd at $E_x = 5418$ keV, compare to a prediction by TRS calculation, assuming a predominantly $\nu(h_{\frac{11}{2}})^2$ configuration of $\beta_2 = 0.17$. A similar value for the β_2 deformation of the $I^\pi = 11^-$ state in ^{106}Cd at $E_x = 4324$ keV has also been deduced. The mean-lifetimes of the yrast $I^\pi = \frac{15}{2}^-$ states in ^{103}Pd and ^{107}Cd have also been deduced. For ^{107}Cd, the mean-lifetime for the yrast $I^\pi = \frac{15}{2}^-$ state at $E_x = 1360$ keV is significantly larger than that reported previously in [44]. The corresponding β_2 value of 0.12(1) compares with the associated β_2 value of 0.14(1) from Häusser *et al.* and a theoretical prediction (from a TRS calculation) of 0.18. In ^{103}Pd, the inferred β_2 deformation of 0.16(1) compares well with the value predicted by TRS calculation of 0.16.

ACKNOWLEDGMENTS

A. Dewald, O. Möller, and P. Petkov are acknowledged by S.F.A. for their assistance with the DDCM analysis. P.H.R. would like to acknowledge financial support from the Yale University Flint Fund and Science Development Fund. This work is supported by EPSRC (UK) and the U.S. DOE, under contract nos. DE-FG02-91ER-40609 and DE-FG02-88ER-40417.

[1] R. F. Casten, N. V. Zamfir, and D. S. Brenner, Phys. Rev. Lett. **71**, 227 (1993).
[2] P. H. Regan *et al.*, Phys. Rev. Lett. **90**, 152502 (2003).
[3] P. H. Regan *et al.*, Phys. Rev. C **68**, 044313 (2003).
[4] P. Cejnar and J. Jolie, Phys. Rev. C **69**, 011301(R) (2004).
[5] P. H. Regan *et al.*, Acta Phys. Pol. B **36**, 1313 (2005).
[6] P. H. Regan *et al.*, Nucl. Phys. **A586**, 351 (1995).
[7] I. Thorslund *et al.*, Nucl. Phys. **A564**, 285 (1993).
[8] I. Thorslund, C. Fahlander, J. Nyberg, M. Piiparinen, R. Julin, S. Juutinen, A. Virtanen, D. Müller, H. Jensen, and M. Sugawara, Nucl. Phys. **A568**, 306 (1994).
[9] M. Piiparinen *et al.*, Nucl. Phys. **A565**, 671 (1993).
[10] S. Juutinen *et al.*, Z. Phys. A **336**, 475 (1990).
[11] S. Juutinen *et al.*, Nucl. Phys. **A573**, 306 (1994).
[12] N. Buforn *et al.*, Eur. Phys. J. A **7**, 347 (2000).
[13] A. J. Simons *et al.*, Phys. Rev. Lett. **91**, 162501 (2003).
[14] A. J. Simons *et al.*, Phys. Rev. C **72**, 024318 (2005).
[15] P. Datta *et al.*, Phys. Rev. C **71**, 041305(R) (2005).
[16] D. C. Stromswold, D. O. Elliott, Y. K. Lee, L. E. Samuelson, J. A. Grau, F. A. Rickey, and P. C. Simms, Phys. Rev. C **17**, 143 (1978).
[17] P. C. Simms, G. J. Smith, F. A. Rickey, J. A. Grau, J. R. Tesmer, and R. M. Steffen, Phys. Rev. C **9**, 684 (1974).
[18] J. A. Grau, F. A. Rickey, G. J. Smith, P. C. Simms, and J. R. Tesmer, Nucl. Phys. **A229**, 346 (1974).
[19] F. A. Rickey, J. A. Grau, L. E. Samuelson, and P. C. Simms, Phys. Rev. C **15**, 1530 (1977).
[20] W. Klamra and J. Rekstad, Nucl. Phys. **A258**, 61 (1976).
[21] D. Jerrestam, F. Liden, J. Gizon, L. Hildingsson, W. Klamra, R. Wyss, D. Barneoud, J. Kownacki, T. Lindblad, and J. Nyberg, Nucl. Phys. **A545**, 835 (1992).
[22] H. A. Smith-Jr and F. A. Rickey, Phys. Rev. C **14**, 1946 (1976).
[23] F. S. Stephens, R. M. Diamond, and S. G. Nilsson, Phys. Lett. **B44**, 429 (1973).
[24] P. J. Nolan and J. F. Sharpey-Schafer, Rep. Prog. Phys. **42**, 1 (1979).
[25] K. Andgren *et al.*, J. Phys. G **31**, S1563 (2005).
[26] K. Andgren *et al.*, AIP Conf. Proc. **831**, 391 (2006).
[27] S. F. Ashley *et al.*, Acta Phys. Pol. B **38**, 1385 (2007).
[28] D. A. Bromley, Nucl. Instrum. Methods **122**, 1 (1974).
[29] C. W. Beausang *et al.*, Nucl. Instrum. Methods Phys. Res. A **452**, 431 (2000).
[30] B. M. Nyakó *et al.*, Phys. Rev. C **60**, 024307 (1999).
[31] R. V. Ribas (private communication).
[32] R. Krücken, J. Res. Natl. Inst. Stand. Technol. **105**, 53 (2000).
[33] J. Theuerkauf, S. Esser, S. Krink, M. Luig, N. Nicolay, O. Stuch, and H. Wolters, computer code TV, unpublished, http://www.ikp.uni-koeln.de/~fitz (1993).
[34] D. Rudolph *et al.*, Phys. Rev. C **65**, 034305 (2002).

[35] K. Lindenberg, F. Neumann, D. Galaviz, T. Hartmann, P. Mohr, K. Vogt, S. Volz, and A. Zilges, Phys. Rev. C **63**, 047307 (2001).
[36] A. Dewald, S. Harissopulos, and P. von Brentano, Z. Phys. A **334**, 163 (1989).
[37] G. Böhm, A. Dewald, P. Petkov, and P. von Brentano, Nucl. Instrum. Methods Phys. Res. A **329**, 248 (1993).
[38] B. Saha, computer code NAPATAU, unpublished.
[39] J. Gableske *et al*., Nucl. Phys. **A691**, 551 (2001).
[40] S. F. Ashley, Ph.D. thesis, University of Surrey (2007).
[41] J. M. Blatt and V. F. Weisskopf, *Theoretical Nuclear Physics* (Dover Publications, New York, 1991).
[42] A. Bohr and B. R. Mottelson, *Nuclear Structure*, Vol. 2: Nuclear Deformation (World Scientific, Singapore, 1998), 2nd edition.
[43] W. Nazarewicz, R. Wyss, and A. Johnson, Phys. Lett. **B225**, 208 (1989).
[44] O. Häusser *et al*., Phys. Lett. **B52**, 329 (1974).
[45] P. Möller, J. R. Nix, W. D. Myers, and W. J. Swiatecki, At. Data Nucl. Data Tables **59**, 185 (1995).
[46] S. Harissopulos, A. Dewald, A. Gelberg, K. O. Zell, P. von Brentano, and J. Kern, Nucl. Phys. **A683**, 157 (2001).
[47] D. D. Frenne and E. Jacobs, Nucl. Data Sheets **93**, 447 (2001).
[48] J. Blachot, Nucl. Data Sheets **91**, 135 (2000).